耶鲁大学-南京信息工程大学大气环境中心
Yale-NUIST Center on Atmospheric Environment

Performance evaluation of an integrated open-path eddy covariance system in a cold desert environment

Wei Wang, Jiaping Xu, Yunqiu Gao, Ivan Bogoev, Jian Cui, Lichen Deng, Cheng Hu, Cheng Liu, Shoudong Liu, Jing Shen, Xiaomin Sun, Liming Wang, Wei Xiao, Guofu Yuan, Xuhui Lee
wangwnuist@163.com

Joint Conference of AsiaFlux Workshop 2017 and the 15th Anniversary Celebration of ChinaFLUX
August, 16-19, 2017
Beijing, China

Outlines

- Unreasonable CO_2 uptake by open-path eddy covariance (EC) system.
  - Self-heating, spectroscopic effect, bias in CO_2 density.
- Lessons learnt from desert IRGASON experiment.
  - Wind statistics, heat fluxes, CO_2 flux.
- Meta-analysis across 64 FLUXNET sites.
- Results

Typical open-path EC system

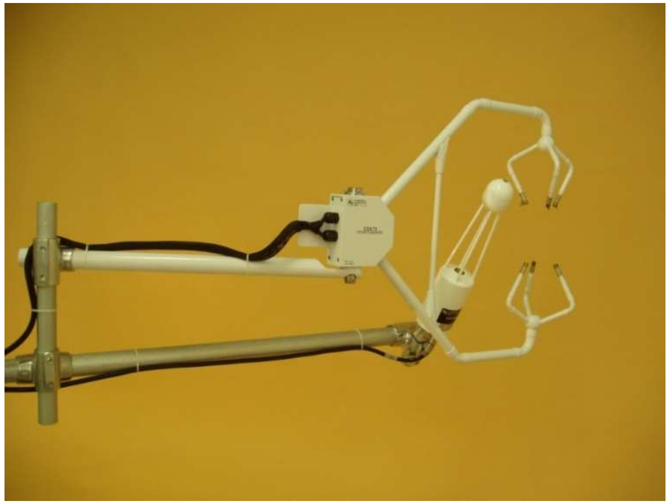

LI-7500/7500A+CSAT3

LI-7500/7500A+Gill

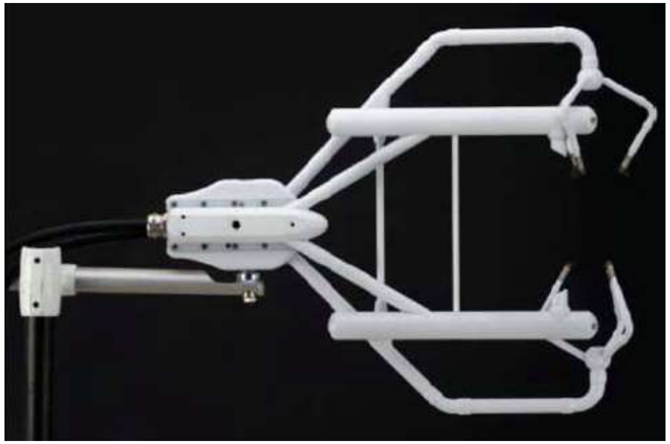

EC150

IRGASON

Physiologically unreasonable CO_2 uptake observed with open-path EC

Period	Landscape	Max (μmol m^{-2} s^{-1})	Mean (μmol m^{-2} s^{-1})	T_a (°C)	Instrument	Reference
19–20 Feb 2005	Burned boreal forest	−5		−12	CSAT3 + LI-7500	Amiro et al. 2006; Amiro 2010
9–10 Jan 2005		−4.2		−23	CSAT3 + LI-7500	Amiro et al. 2006
Jan 2003	Temperature larch forest	−3		−5	TR-61C + LI-7500	Hirata et al. 2007
Jan 2002–Dec 2004	Boreal evergreen forest	−3		−20	CSAT3 + LI-7500	Welp et al. 2007
Jan 2002–Dec 2004	Boreal deciduous forest	−2		−20	CSAT3 + LI-7500	Welp et al. 2007
27 days in late winter, 2004	Low arctic tundra	−0.9		−10	Gill R3-50 + LI-7500	Lafleur and Humphreys 2008
9–11 Apr 2003	Drained paddy field	−5.9		12	SAT + LI-7500	Ono et al. 2008
Winter, 2005–07	Mojave Desert		−0.3 (daily)	−2	CSAT3 + LI-7500	Wohlfahrt et al. 2008
Oct–Dec 2006	Beech forest	−2		0 to 12	Gill R2 + LI-7500	Järvi et al. 2009
Jan 2007	Mediterranean alpine shrubland	−2		3	Metek USA-1 + LI-7500	Reverter et al. 2010
Winter, 2006–08	Eucalyptus plantation	−10	−5 (daily)	15 to 25	CSAT3 + LI-7500	Cabral et al. 2011
1 Nov 2007–31 Jan 2008	Arctic polyn'ya	−27.95	−4.88 (whole period)	−7.5 to −25	Gill WindMaster Pro + LI-7500	Else et al. 2011
Winter, 2003–09	Alpine meadow	−6		0 to −10	Gill R3 + LI-7500	Marcolla et al. 2011
1 Jan–1 Jun 2004	Sea ice	−14	−0.7 (daily)	0 to −35	CSAT3 + LI-7500	Miller et al. 2011
Winter, 2006–10	Urban area	−5		−10	Metek USA-1 + LI-7500	Järvi et al. 2012
May–Oct 2008	Subarctic tundra	−4	−0.48 (daily)	−3.5	Gill R3 + LI-7500	Marushchak et al. 2013
Jan 2005–11	Sea kelp beds	−8	−4.6 (daily)	11	CSAT3 + LI-7500	Ikawa and Oechel (2015)
Winter, 2008–12	Blanket bog		−0.5 (daily)	−3	CSAT3 + LI-7500	Lund et al. 2015

Wang et al., 2016, JTECH

Three possible explanations for unreasonable CO_2 uptake

- Self-heating: additional heat generated by the instrument electronics or by the solar loading (Burba et al., 2008), such as LI-7500 .
- Spectroscopic effects: attenuation of temperature at high frequencies and spectroscopic cross-sensitivity (Detto et al., 2011; McDermitt et al., 2011; Bogoev et al., 2014), such as EC150 and IRGASON.
- Errors propagation through density correction procedure by bias in CO_2 density (Serrano-Ortiz et al., 2008; Fratini et al., 2014), all IRGAs.

Self-heating of open-path EC

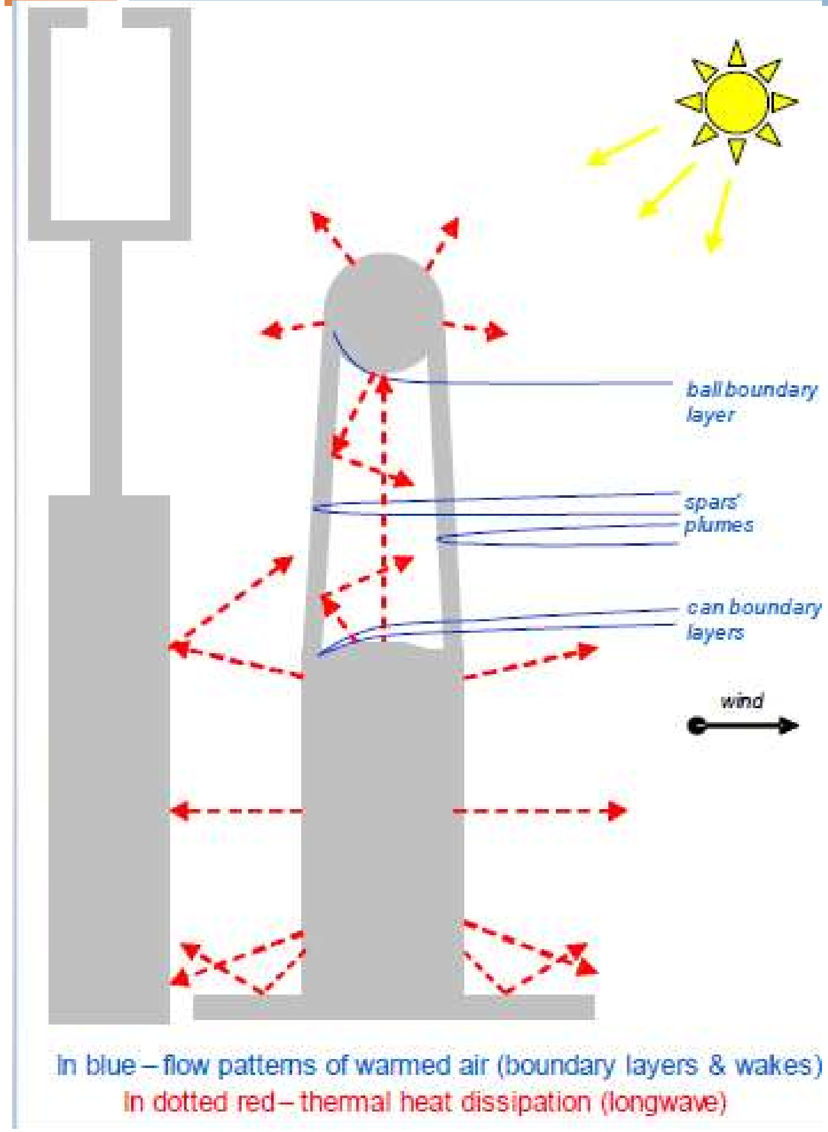

- First interval: low wind, $U'<0$, $U'w'<0$, then $w'>0$, surface warming, air expansion, $CO_2'<0$, then $w'CO_2'<0$, artificial CO_2 uptake.

- Second interval: strong wind, $U'>0$, $U'w'<0$, then $w'<0$, less surface warming, smaller air expansion, $CO_2'\approx 0$, no artificial CO_2 uptake.

Burba and Anderson, 2010

Theoretical consideration of self-heating

- WPL density correction algorithm (Webb et al., 1980)

$$F_c = \overline{w'\rho_c'} + \frac{\overline{\rho_c}}{\overline{T}C_p\overline{\rho_a}}\left(1 + \frac{\overline{\rho_v}M_a}{\overline{\rho_a}M_v}\right)H + \frac{\overline{\rho_c}M_a}{\overline{\rho_a}M_v}\lambda E$$

$$F_c' = \overline{w'\rho_c'} + \frac{\overline{\rho_c}}{\overline{T}C_p\overline{\rho_a}}\left(1 + \frac{\overline{\rho_v}M_a}{\overline{\rho_a}M_v}\right)(H + \delta H) + \frac{\overline{\rho_c}M_a}{\overline{\rho_a}M_v}\lambda E$$

$$F_c = F_c' + bH$$

$$b = -\frac{\overline{\rho_c}}{\overline{T}C_p\overline{\rho_a}}\left(1 + \frac{\overline{\rho_v}M_a}{\overline{\rho_a}M_v}\right)\frac{\delta H}{H}$$

$\frac{\delta H}{H} = 0.14$ (Burba et al., 2008), b is -0.007 μmol m^{-2} s^{-1} per W m^{-2}.

Wang, Lee, Lin, et al., in review

Spectroscopic effect due to high-frequency temperature attenuation

$$A = \frac{N}{(\Delta \nu)} \int_{\nu_1}^{\nu_2} \left\{ 1 - \exp\left(- \frac{S_i \alpha_i C L}{\pi \left[\left(\nu - \nu_{0i} \right)^2 + \alpha_i^2 \right]} \right) \right\} d\nu$$

$$S_i = f_1(T,P) \;\; \alpha_i = f_2(T,P) \qquad \alpha_i(P,T) = \alpha_0 \frac{P}{P_0} \left(\frac{T_0}{T} \right)^{1/2}$$

Jamieson et al. 1963

$$F_c' = F_c + 0.014257H - 0.066828$$

Bogoev et al. , 2015

Theoretical consideration of spectroscopic effect

$$\alpha = \tilde{\alpha} + \Delta\alpha, \tilde{\alpha} = \alpha_o \frac{P}{P_o}\left(\frac{T_o}{\tilde{T}}\right)^{1/2}$$

$$\Delta\alpha = -\frac{1}{2}\,\tilde{\alpha}\,\frac{T'}{\tilde{T}}$$

$$\Delta A = -\tilde{A}\,\frac{\Delta\alpha}{\tilde{\alpha}} = \tilde{A}\,\frac{1}{2}\,\frac{T'}{\tilde{T}}, \qquad A = \tilde{A}\left(1 + \frac{1}{2}\frac{T'}{\tilde{T}}\right)$$

$$C = \tilde{C}\left(1 + \frac{1}{2}\frac{T'}{\tilde{T}}\right)$$

$$F_c' \approx F_c + \frac{1}{2}\,\frac{1}{\rho c_p}\,\frac{\bar{C}}{\bar{\bar{T}}}\,H$$

Wang et al., 2016, JTECH

$$F_c = F_c' + bH$$

$$b = -\frac{1}{2}\,\frac{1}{\rho c_p}\,\frac{\bar{C}}{\bar{\bar{T}}} \approx -0.025\ \mu\text{mol m}^{-2}\ \text{s}^{-1}$$

$$b \approx -0.014\ \mu\text{mol m}^{-2}\ \text{s}^{-1}$$

Universal negative linear relationship between F_c and H

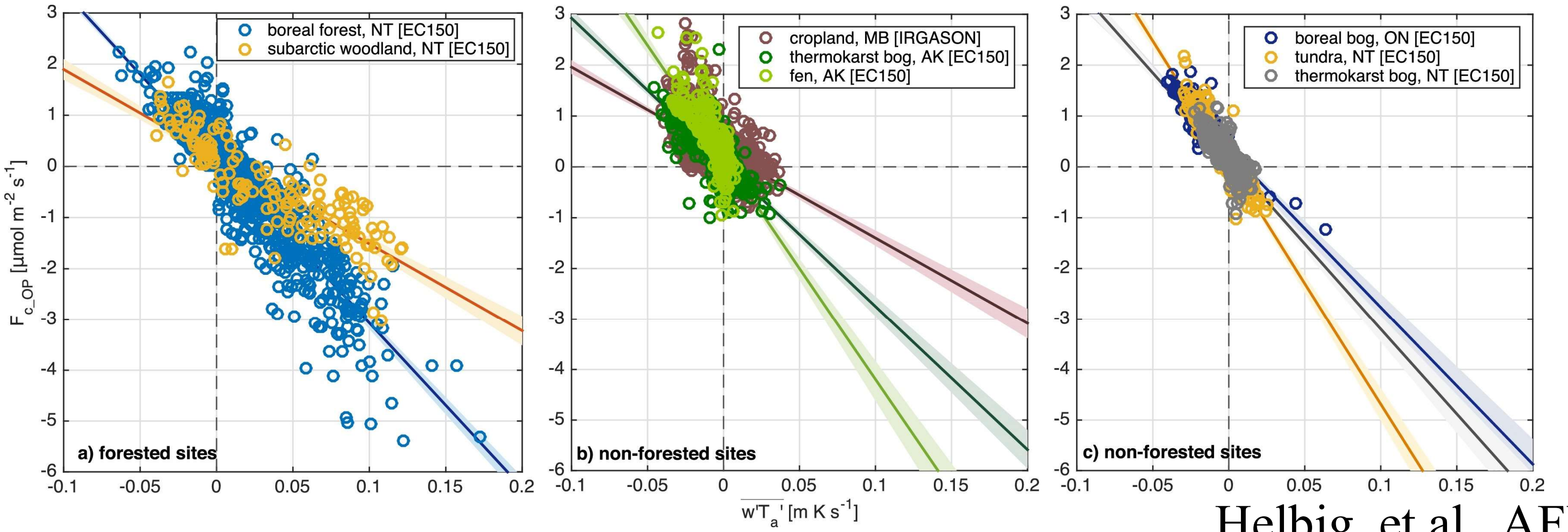

Helbig, et al., AFM, 2016

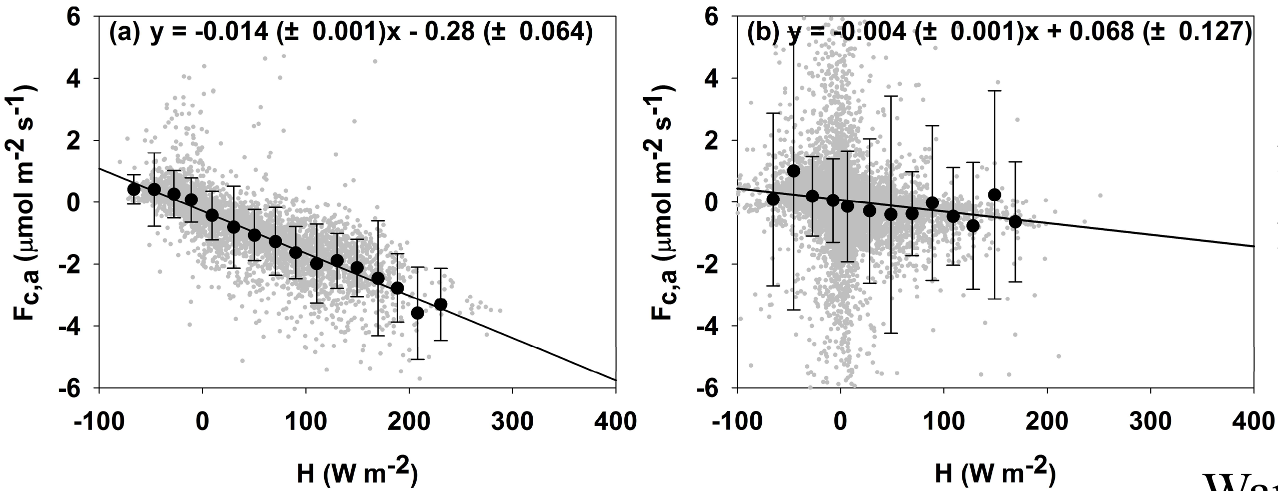

Significant and negative linear relationship existed at **37 sites** across 64 FLUXNET sites.

Wang, Lee, Lin, et al., in review

Theoretical consideration of bias CO_2 density

$$F_c = \overline{w'\rho_c'} + \frac{(\overline{\rho_c} + \delta\overline{\rho_c})}{\overline{\overline{T}}C_p\overline{\rho_a}}\left(1 + \frac{\overline{\rho_v}M_a}{\overline{\rho_a}M_v}\right)H + \frac{(\overline{\rho_c} + \delta\overline{\rho_c})M_a}{\overline{\rho_a}M_v}\lambda E$$
$$= F_c' + bH$$

$$b = \frac{\delta\overline{\rho_c}}{\overline{\overline{T}}C_p\overline{\rho_a}}\left(1 + \frac{\overline{\rho_v}M_a}{\overline{\rho_a}M_v}\right)\left(\frac{\delta\overline{\rho_c}}{\overline{\rho_c}}\right) \approx 0.05\frac{\delta\overline{\rho_c}}{\overline{\rho_c}}$$

- Across 64 sites, $\frac{\delta\overline{\rho_c}}{\overline{\rho_c}}$ = -5%, *b* is about -0.0025 μmol m^{-2} s^{-1} per W m^{-2}.

Wang, Lee, Lin, et al, in review

Hypothesis

- Integrating the infrared gas analyzer's sensing heads into the sensing volume of the sonic anemometer has negligible effects on dynamic flows of the IRGASON.

- Inadequate spectroscopic correction by slow response air temperature measurement partly contribute to ecologically unreasonable CO_2 uptake with IRGASON.

Site (cold arid desert) and Instrumentation

Instrument	Sensor	Height/depth (m)	Variables	Operation period
EC	LI-7500A (LI-COR, Inc.) + WindMaster Pro (Gill Instruments Ltd.)	15	H, λE, F_c, u_*, T_s, CO_2, ρ_v,	Jun 2013–10 Mar 2014
	IRGASON (Campbell Scientific, Inc.)	15	u, v, w, U, wind direction	16 Dec 2013–3 Jan 2014; 12 Mar 2014–13 Apr 2014
Radiation	CNR4 (Kipp and Zonen B.V.)	14	$K_\downarrow$, $K_\uparrow$, $L_\downarrow$, $L_\uparrow$, R_n	Jun 2013–now
	PAR LITE (Kipp and Zonen B.V.)	14	PAR	Jun 2013–now
Micrometeorology	HMP155A (Vaisala Inc.)	11, 14	T_a, RH	Jun 2013–now
	SI-111 (Apogee Instruments, Inc.)	11	Surface temperature	Jun 2013–now
	TE525MM (Campbell Scientific, Inc.)	11	Precipitation	Jun 2013–now
Soil	Hukseflux HFP01 (Hukseflux Thermal Sensors B.V.)	0.08, 0.2, 0.5	Soil heat flux	Jun 2013–now

Period	Date	*Populus* trees	T_a (°C)	ρ_v (ppm)	$K_\downarrow$ (W m^{-2})	Albedo
Winter	Dec.16, 2013-Jan.3, 2014,	dormant season	-6.7	2730	91.1	0.28
Spring	Mar.12, 2014-Apr.13, 2014	flowering stage	14.1	3390	195.0	0.27

Wind statistics

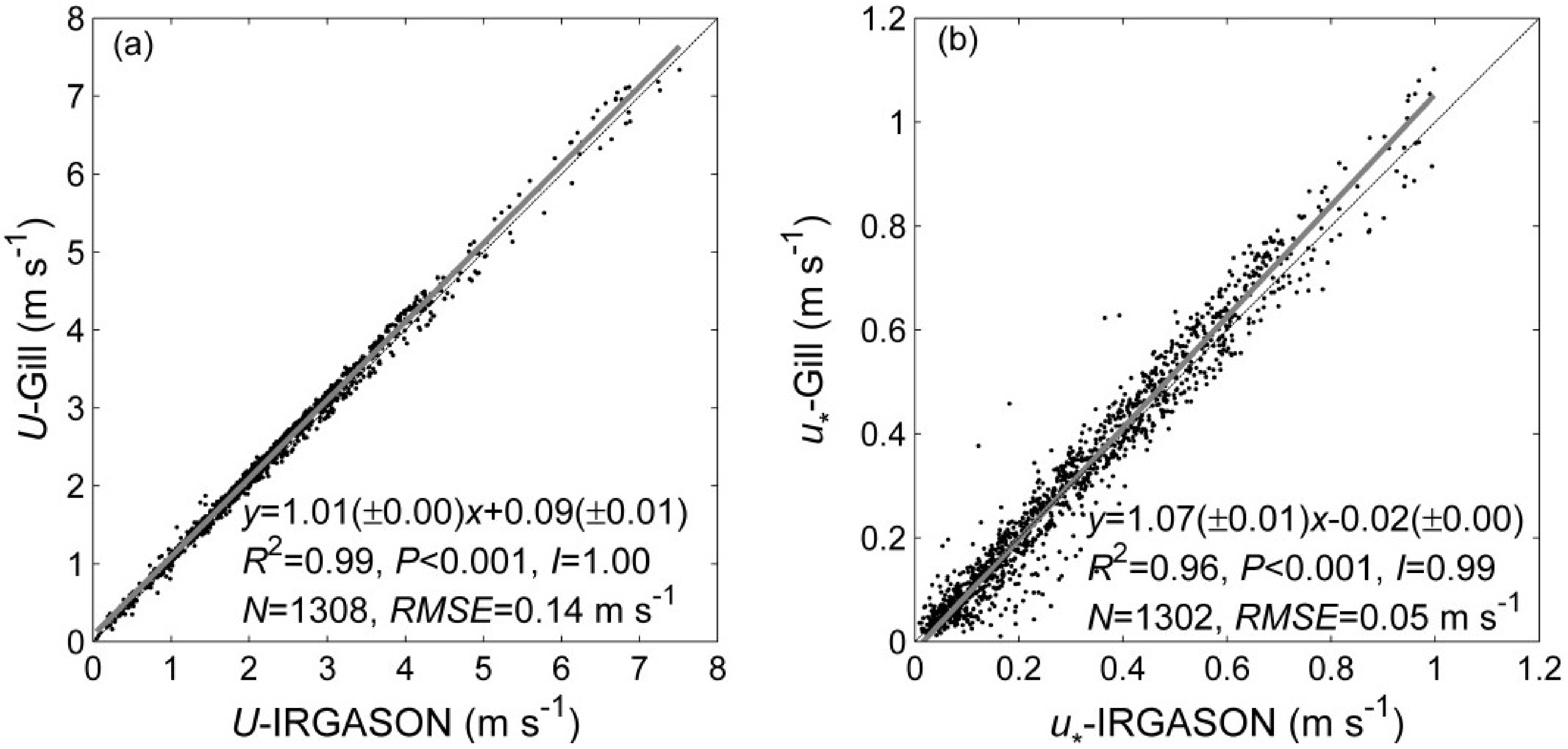

Wang et al., 2016, JTECH

The Monin-Obukhov scaling relationships

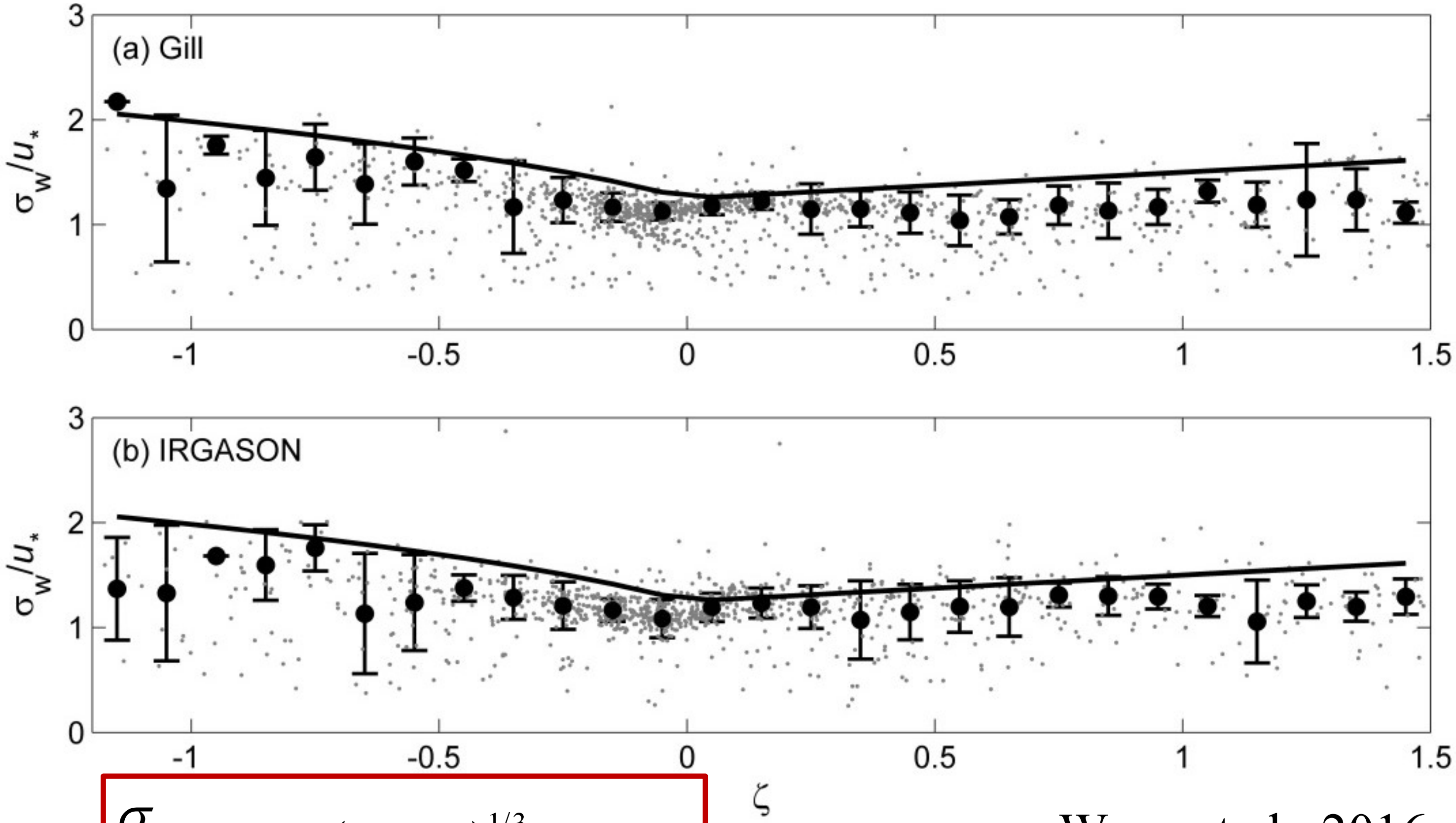

$$\frac{\sigma_w}{u_*} = 1.25(1-3\xi)^{1/3} \quad \xi < 0$$

$$\frac{\sigma_w}{u_*} = 1.25(1+0.2\xi) \quad \xi > 0$$

Wang et al., 2016, JTECH

Garratt 1992; Kaimal and Finnigan 1994

Spectral and cospectral analysis

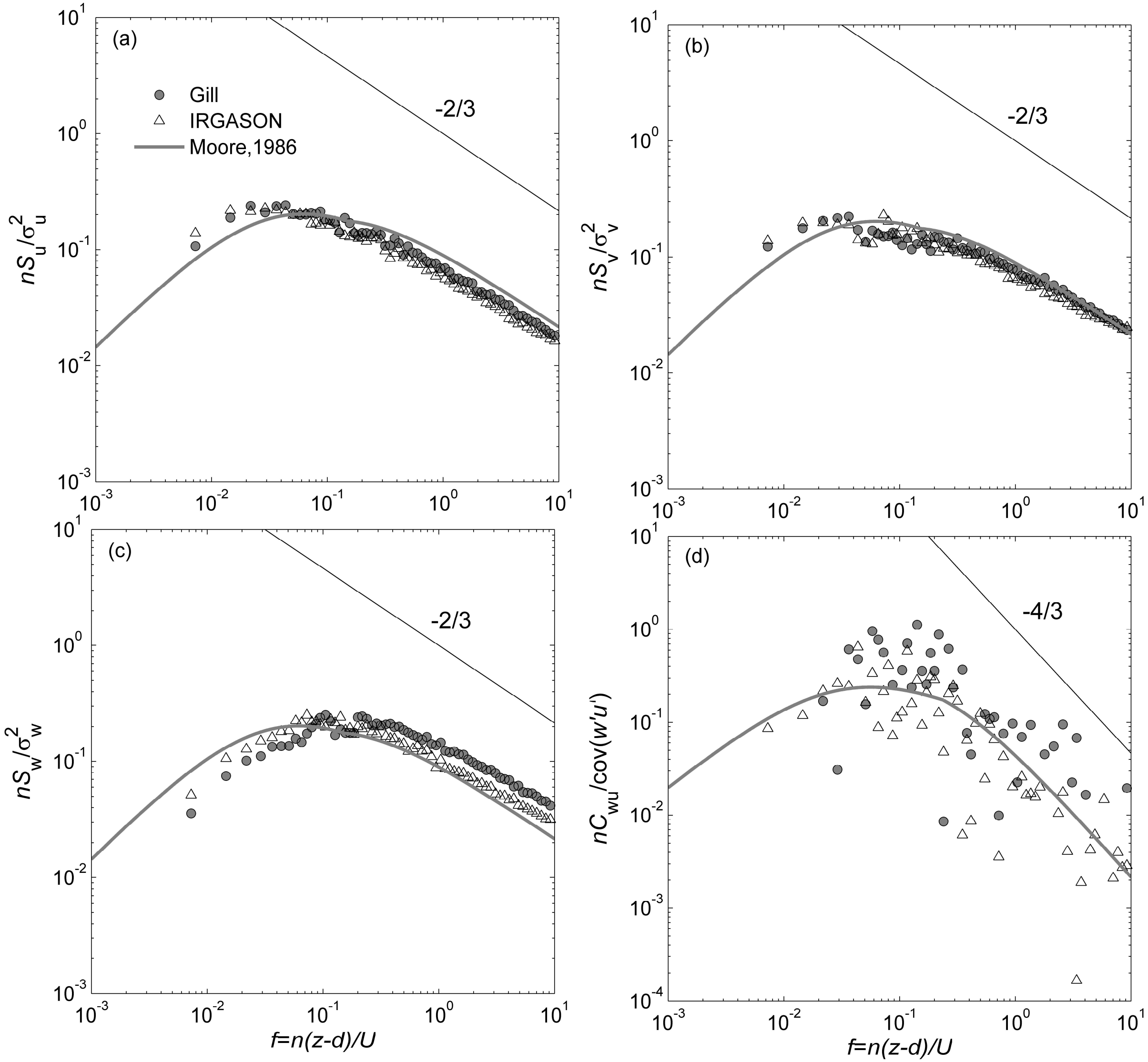

Wang et al., 2016, JTECH

Sensible and latent heat flux

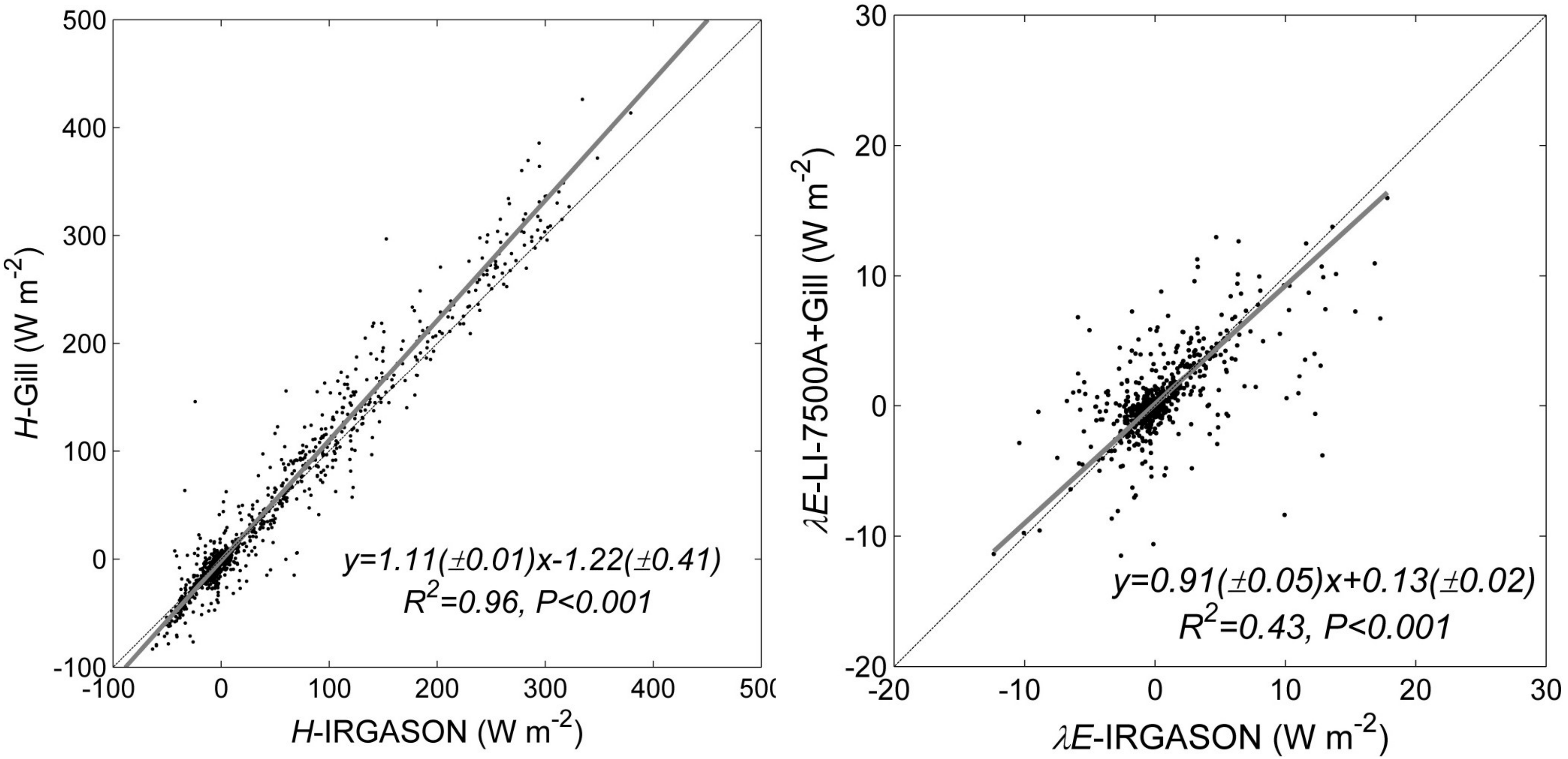

Wang et al., 2016, JTECH

CO_2 flux time series

$$F_c' = F_c + 0.014257H - 0.066828$$

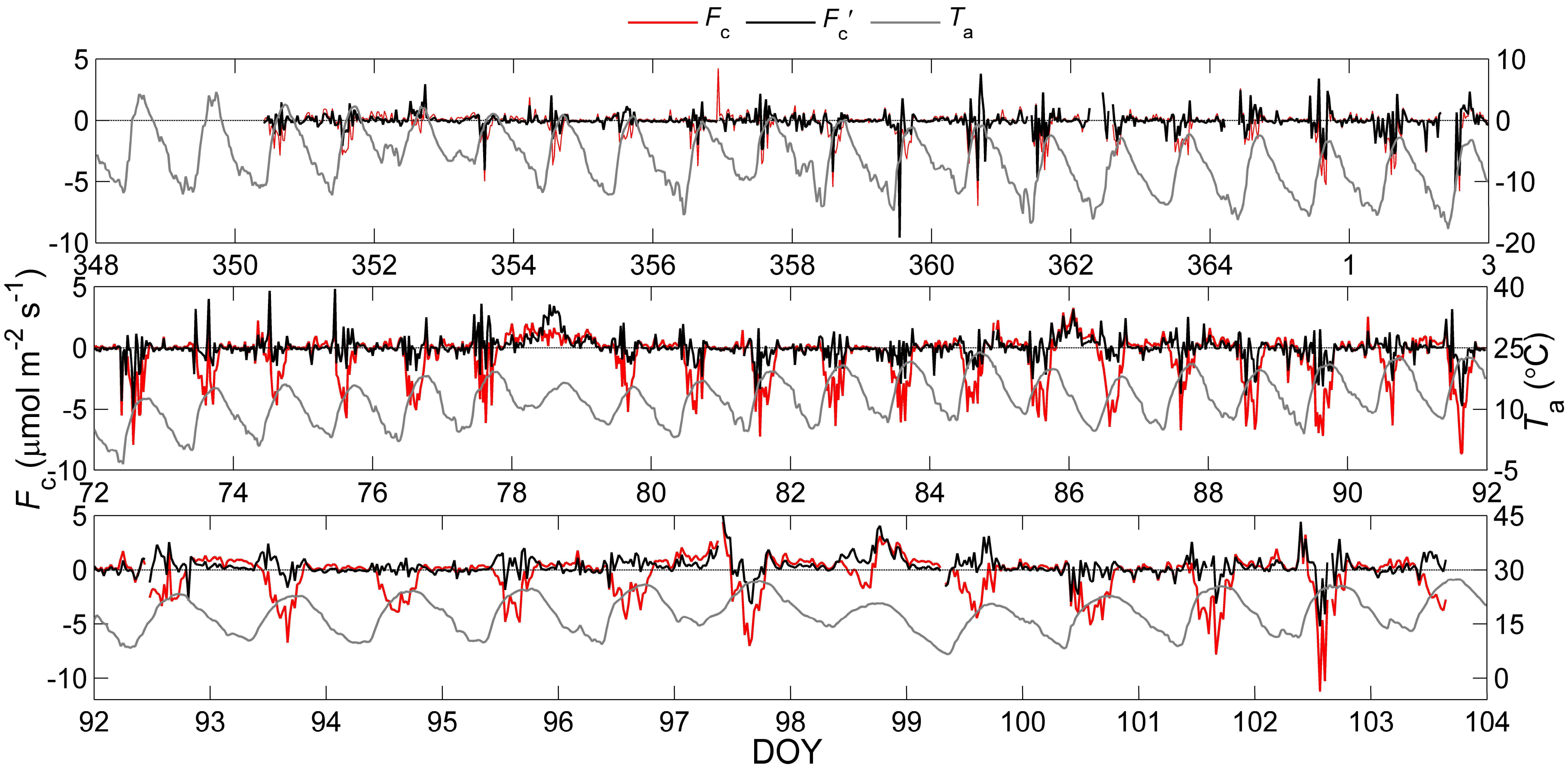

- Winter mean F_c was -0.25 μmol m^{-2} s^{-1} and -0.22 μmol m^{-2} s^{-1} for the separated EC system and the IRGASON, respectively.

Wang et al., 2016, JTECH

Diurnal composition of CO_2 flux in winter

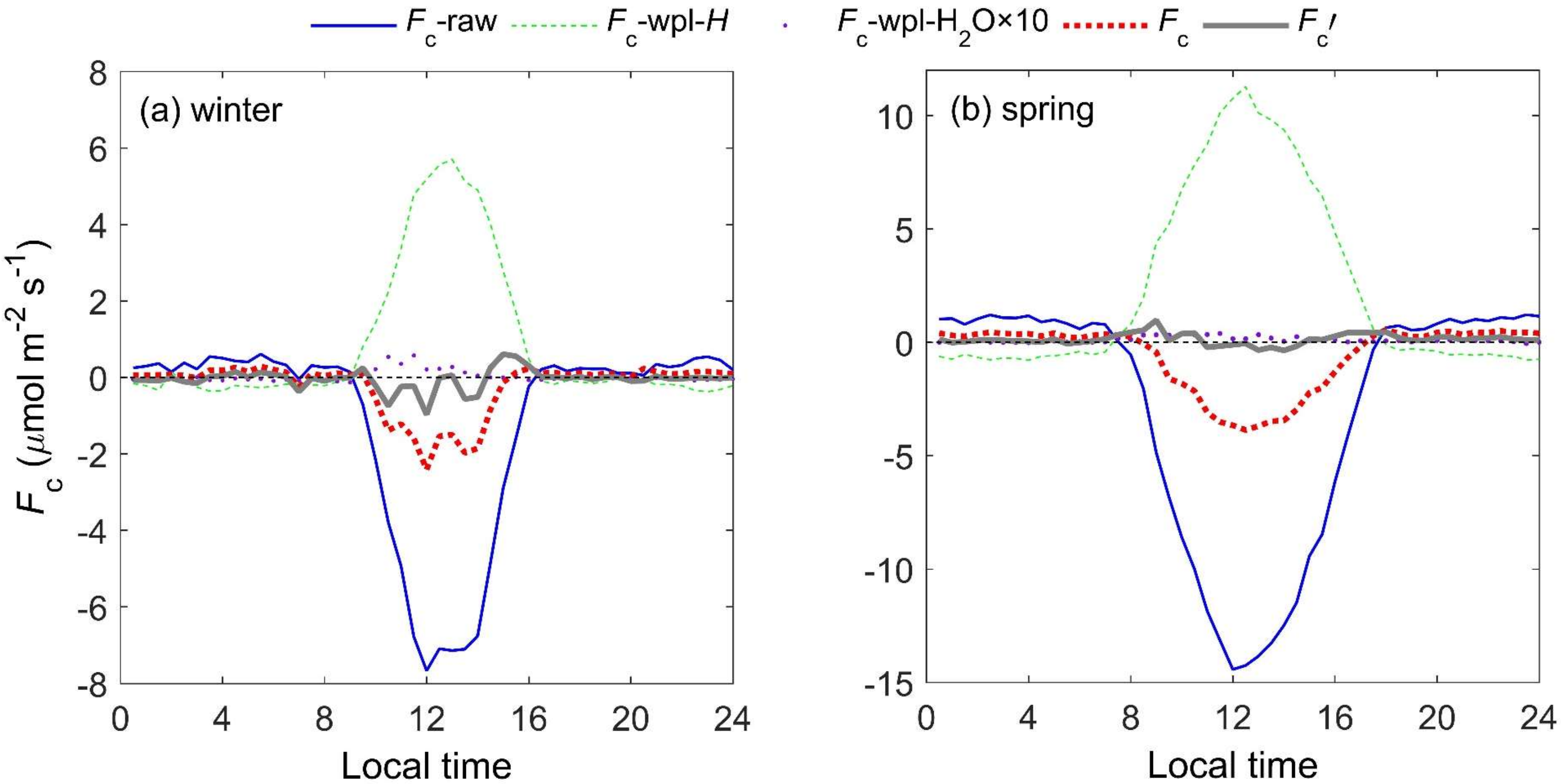

- After applying correction for spectroscopic effect, the wintertime IRGASON CO_2 flux became physiologically reasonable (mean value -0.04 μmol m^{-2} s^{-1}). Wang et al., 2016, JTECH

Comparison among three gas analyzer types

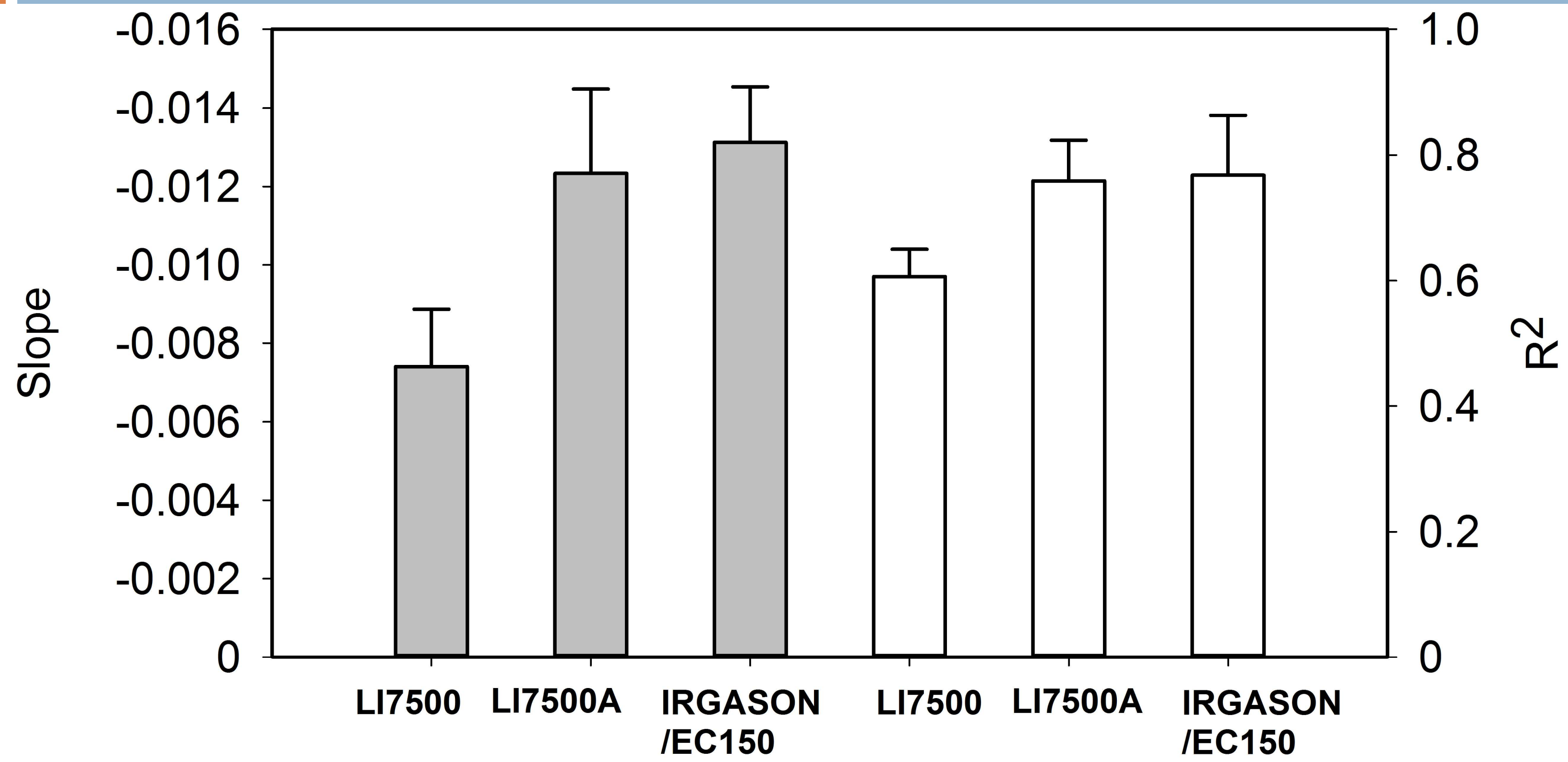

- The slope parameter *b* (μmol m^{-2} s^{-1} per W m^{-2}; gray bars) and the R^2 value (white bars) of the linear regression between wintertime F_c and H. Error bars are ±1 standard error.

Wang, Lee, Lin, et al, in review

Comparison among geographic regions

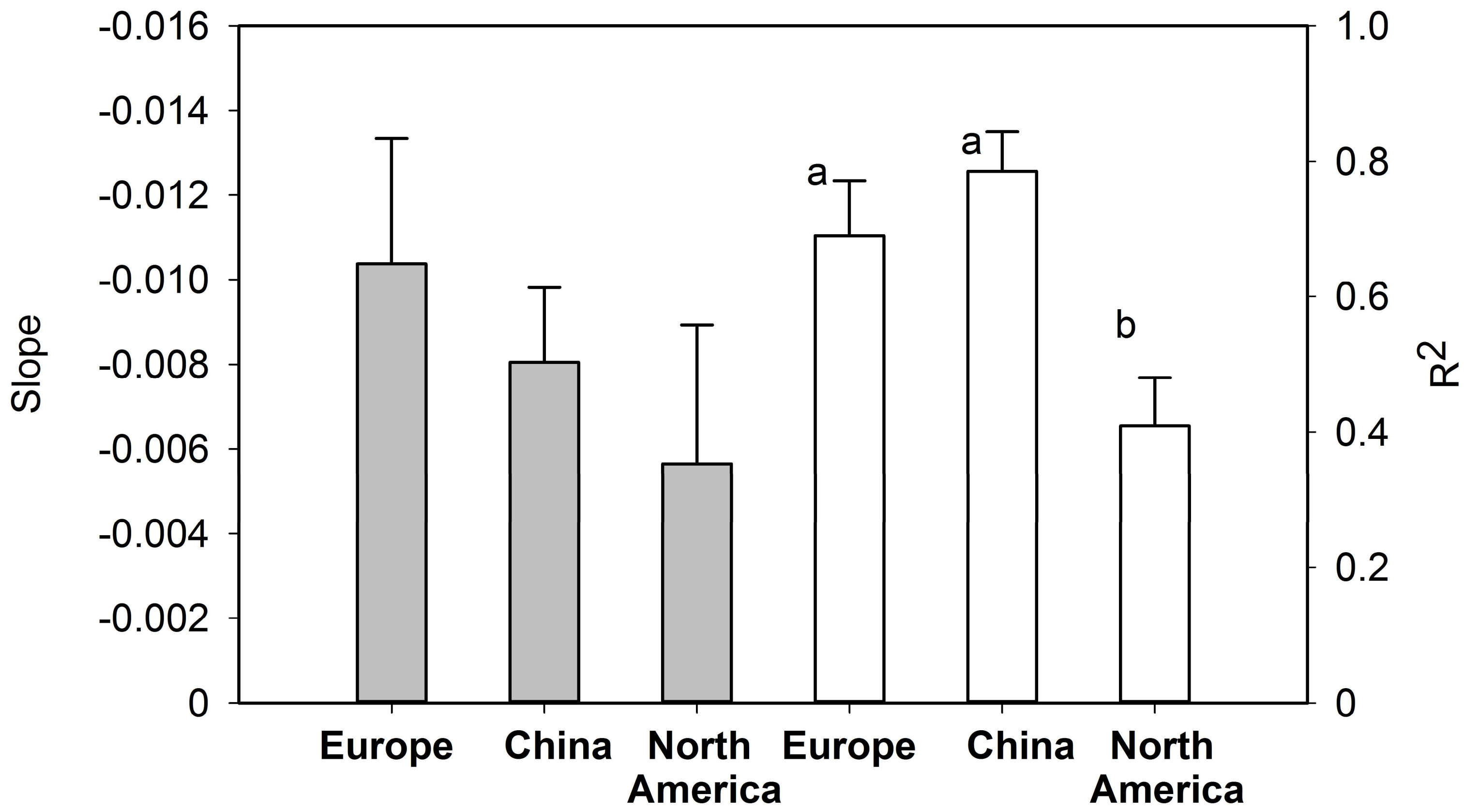

Wang, Lee, Lin, et al, in review

Conclusions

- Integrating an IRGA into measuring volume of the IRGASON sonic anemometer had negligible effects on its wind statistics.
- Both EC systems observed negative CO_2 fluxes (-1.6 µmol m^{-2} s^{-1}) in the daytime during the winter experiment. Sensor self-heating was ruled out as the cause of the apparent uptake flux.
- After applying correction for spectroscopic effect, the wintertime IRGASON CO_2 flux became physiologically reasonable (mean value -0.04 µmol m^{-2} s^{-1}).
- The negative linear relationship between observed CO_2 flux and sensible heat flux is universal and was confirmed by a meta-analysis of open-path EC data from 64 FLUXNET sites.

Related papers

- Bogoev, I., 2014: Improved eddy flux measurements by open-path gas analyzer and sonic anemometer co-location. *Geophysical Research Abstracts*, Vol. 16, Abstract EGU2014-199.
- Wang, W., et al., 2016: Performance evaluation of an integrated open-path eddy covariance system in a cold desert environment. *Journal of Atmospheric and Oceanic Technology*, 33(11): 2385–2399.
- Helbig, M., et al., 2016: Addressing a systematic bias in carbon dioxide flux measurements with the EC150 and the IRGASON open-path gas analyzers. *Agricultural and Forest Meteorology*, 228: 349-359.
- Wang, L.M., et al., 2017: A meta-analysis of eddy covariance observations of apparent CO_2 uptake in cold conditions in the FLUXNET network. In review.

Data sharing http://yncenter.sites.yale.edu

yncenter.sites.yale.edu/data-access

Yale-NUIST Center on Atmospheric Environment

Science Team | Publication | Presentation | Video Conference | Meeting | Gallery | Project | Data

Thanks for your attention!

Data Access

Follow the link to download the data and the readme file. If you plan to use our data for journal publication, please contact Ms. Zhen Xu at 478766329@qq.com. We will let you know if your plan conflicts with ours and if we should be offered coauthorship.

1) Micrometeorology, water temperature, and radiation and heat fluxes at Meiliangwan, Lake Taihu (2010-2011)

Languages

English
简体中文